

## Supporting Information

# Heterostructure Engineering of N-doped NiMoO<sub>4</sub> Two-Phase Electrocatalyst for Industrial Large-scale Synthesis of 2, 5-Furan Dicarboxylic Acid

*Ximin Zhang, Ao Wang, Wenbiao Wang, Gang Xu, Shijiao Dong, Meiqing Cai and Jun-Ling Song\**

E-mail:s070054@e.ntu.edu.sg

International Joint Research Center for Photoresponsive Molecules and Materials,  
School of Chemical and Material Engineering, Jiangnan University, Lihu Street 1800,  
Wuxi 214122, China

### Experimental section

**Reagents and materials:** All reagents used in this study were purchased and directly used without further purification: Ni(NO<sub>3</sub>)<sub>2</sub>·6H<sub>2</sub>O(AR) and (NH<sub>4</sub>)<sub>6</sub>Mo<sub>7</sub>O<sub>24</sub>·4H<sub>2</sub>O(AR) were purchased from Shanghai Titan Scientific Co., Ltd.. Nickel foam (NF) was purchased from Suzhou Cheng Er Nuo Technology Co. Ltd.

**Physical characterizations:** The structure of N-NiMoO<sub>4</sub>/NF is determined by PXRD (Bruker D8, Cu-Kα). the spectra were recorded in the 2θ range of 5° to 60°. The morphology of Ni-Mo-S were investigated by scanning electron microscopy (SEM, Hitach S-4800) and transmission electron microscope (TEM, JEOL 2100F). X-ray electron spectroscopy (XPS) was performed on AXIS Supra by Kratos Analytical Inc. Using monochromatized Al Kα radiation as X-ray source. All spectra were calibrated

by C 1s (284.8 eV).

### **Product analysis:**

The concentrations of HMF and oxidation products were determined by high performance liquid chromatography (HPLC) system (Waters 1525) using a  $4.6 \times 250$  mm NuovaSil C18-WH,  $5\mu\text{m}$  column with detection wavelength set at 265 nm and column temperature maintained at  $30\text{ }^{\circ}\text{C}$ . The HPLC eluent was a mixture of solvent A (5 mM ammonium formate solution) and B (methanol). For the HMF oxidation reaction, isocratic elution separation was performed using 30% A and 70% B at a flow rate of  $0.6\text{ mL min}^{-1}$  over 15 min. HPLC samples were prepared by diluting 1.0 mL of the reaction mixture with 49.0 mL of deionized water. Quantification of HMF and oxidation products was calculated from the calibration curve. The HMF conversion, the product yield, and the FE value of FDCA were calculated using the following equations, where F is Faraday's constant.

The conversion of HMF can be calculated by the following eqn:

$$\text{Conversion} = \frac{n(\text{reacted HMF})}{n(\text{initial HMF})} \times 100\%$$

The selectivity and yield of the FDCA were determined by the following eqn respectively:

$$\text{Selectivity} = \frac{n(\text{FDCA production})}{n(\text{reacted HMF})} \times 100\%$$

$$\text{Yield} = \frac{n(\text{FDCA production})}{n(\text{initial HMF})} \times 100\%$$

The faradaic efficiency of the product was calculated using eqn:

$$\text{FE of FDCA} = \frac{\text{mol of FDCA formed}}{\text{total charge passed}/(6 \times F)} \times 100\%$$

**Electrochemical measurements:** All electrochemical tests were carried out in a three-electrode system using a CHI760E electrochemical workstation (Shanghai Chenhua, China) without iR correction. HMFOR and OER were carried out in a typical three-electrode system with a H-type cell separated by an anion exchange membrane (N117 DuPont). Pt wire and Hg/HgO were used as counter electrode and reference electrode, the as-prepared N-NiMoO<sub>4</sub>/NF ( $1\text{cm} \times 1\text{cm}$ ) material was used as the working electrode. The measured voltage value is converted into the electrode potential vs the

reversible hydrogen electrode (RHE) by the equation  $E_{\text{RHE}} = E_{\text{Hg/HgO}} + 0.059 \times \text{pH} + 0.098$  V. The electrochemical OER and HMFOR experiments were conducted in 50 mL of 1.0 M NaOH solution with and without 20 mM. Electrochemical impedance spectroscopy (EIS) measurements were recorded in the frequency range of  $10^5$ –0.1 Hz with an amplitude of 5 mV. The electric double layer capacitance of the prepared catalyst was determined by the CV of different scanning speeds (20, 40, 60, 80 and 100  $\text{mV s}^{-1}$ ).

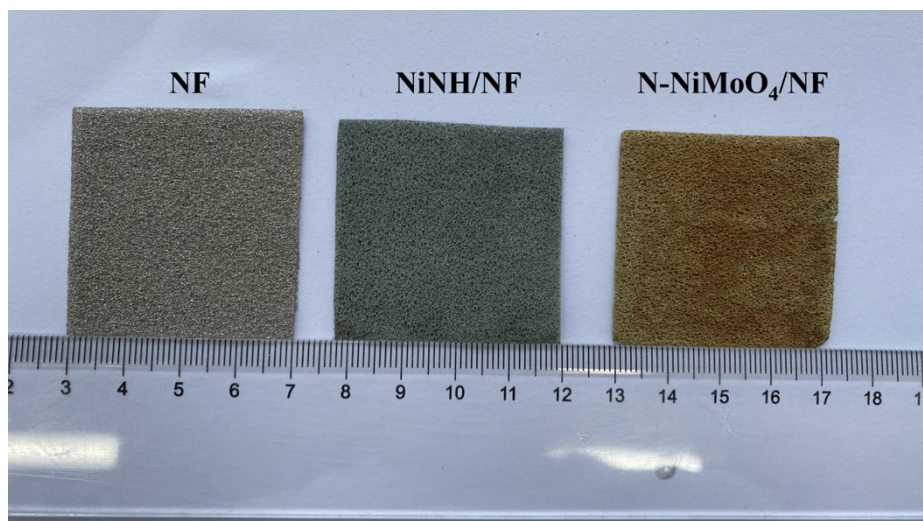


**Figure S1** Photograph of bare NF (left), NiNH NF (middle), and N-NiMoO<sub>4</sub>/NF (right).

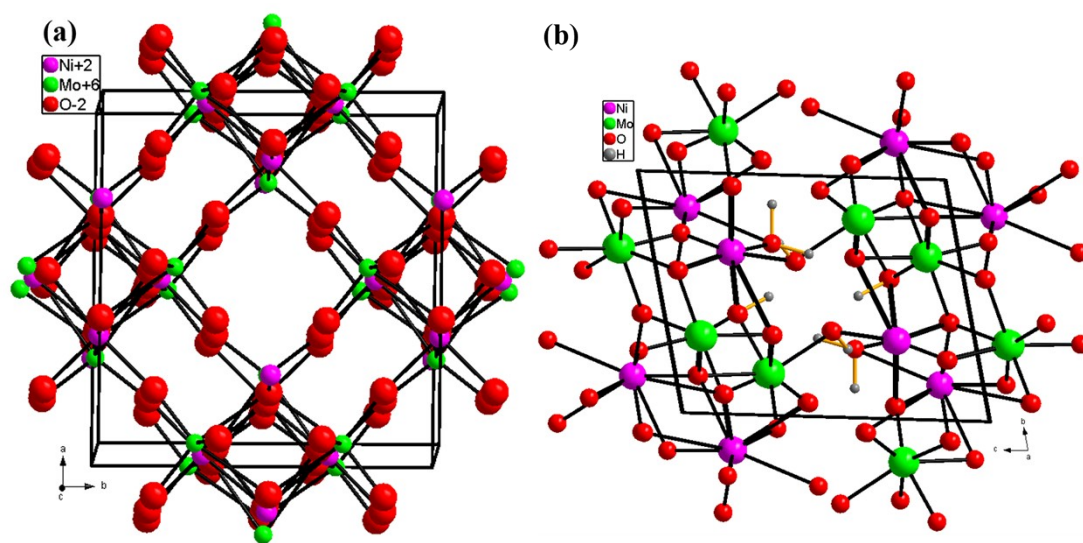


**Figure S2** The crystal structure of  $\text{NiMoO}_4$  (a) and  $\text{NiMoO}_4 \cdot \text{H}_2\text{O}$  (b).

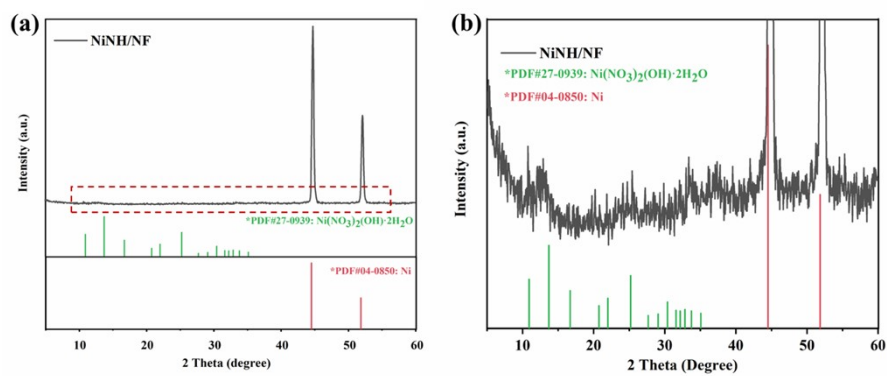


**Figure S3** XRD patterns of  $\text{NiNH/NF}$  (a) and the expanded view of PXRD of  $\text{NiNH/NF}$ .

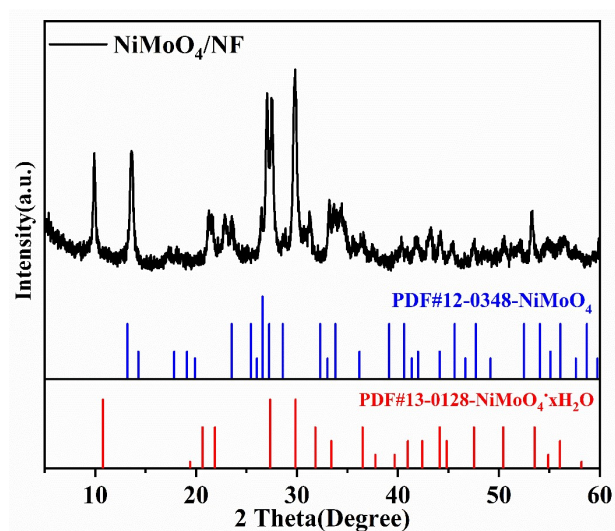


**Figure S4** XRD patterns of NiMoO<sub>4</sub>/NF.

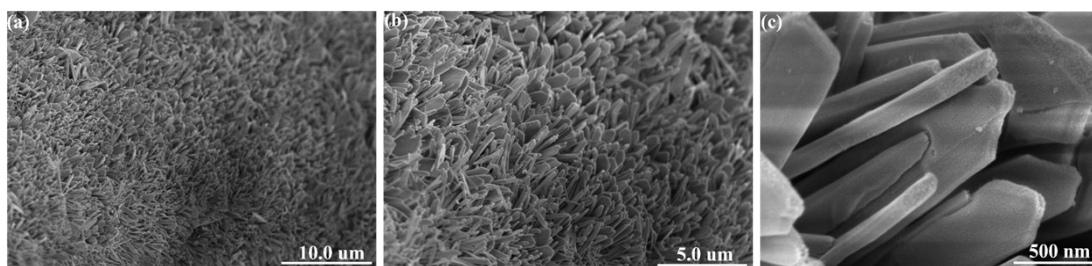


**Figure S5** (a-c) SEM images of NiNH/NF.

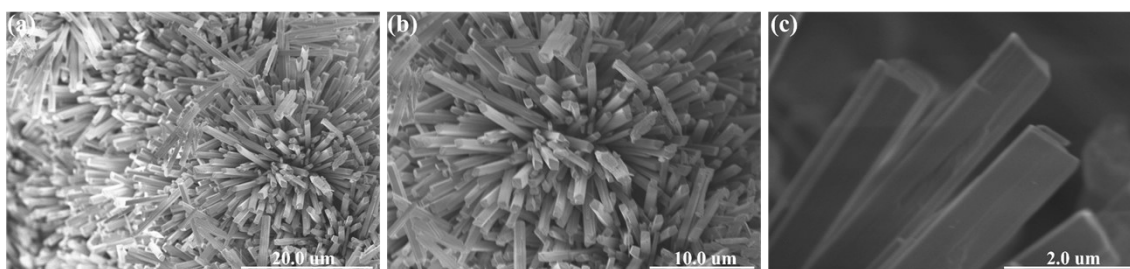


**Figure S6** SEM images of NiMoO<sub>4</sub>/NF.

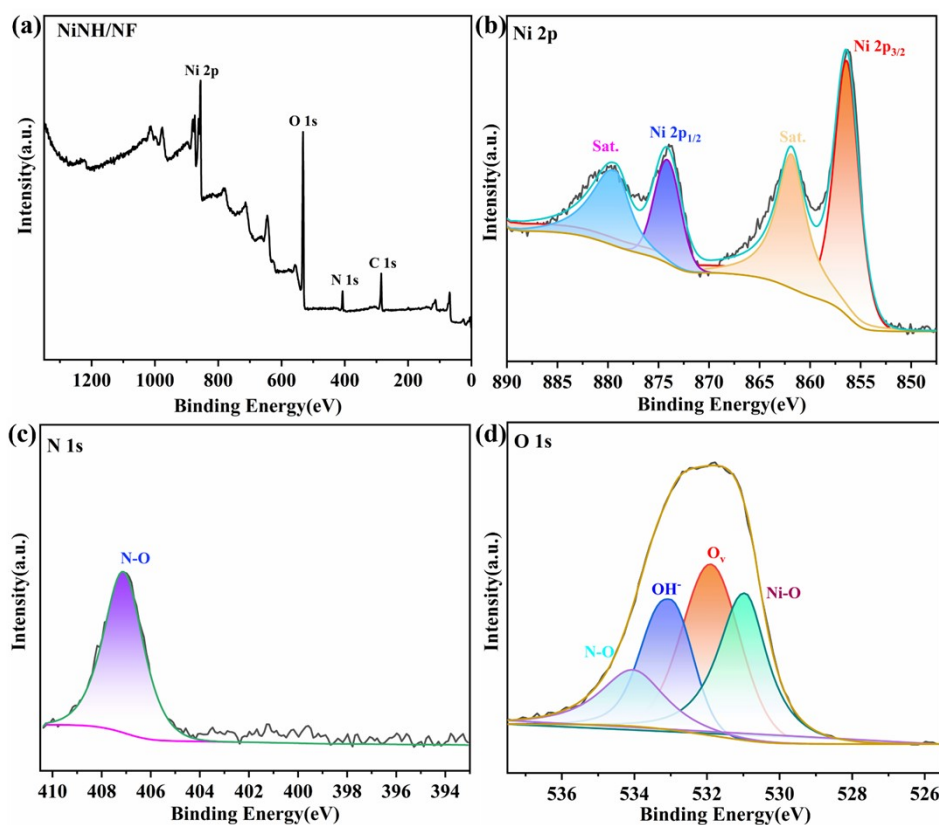


**Figure. S7** XPS spectra of Survey full spectra(a), Ni 2p (b), N 1s (c) and O 1s (d) of NiNH/NF.

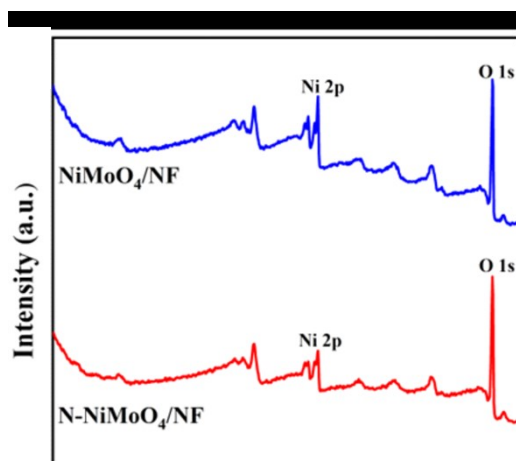


**Figure. S8** High-resolution XPS spectra for NiMoO<sub>4</sub>/NF and N-NiMoO<sub>4</sub>/NF of survey spectra

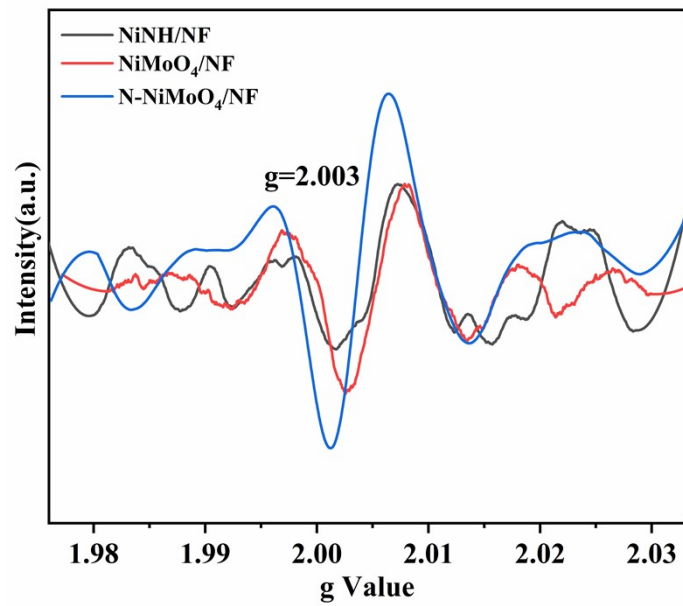


**Figure. S9** EPR spectra of NiNH/NF, NiMoO<sub>4</sub>/NF and N-NiMoO<sub>4</sub>/NF.

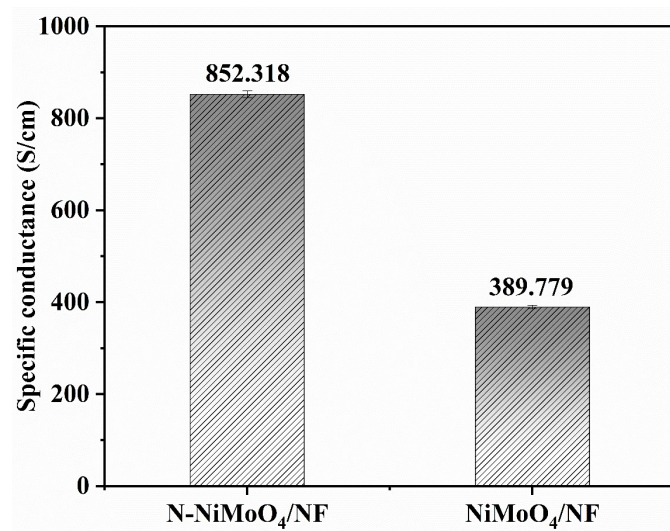


**Figure. S10** Conductivity of N-NiMoO<sub>4</sub>/NF and N-NiMoO<sub>4</sub>/NF.



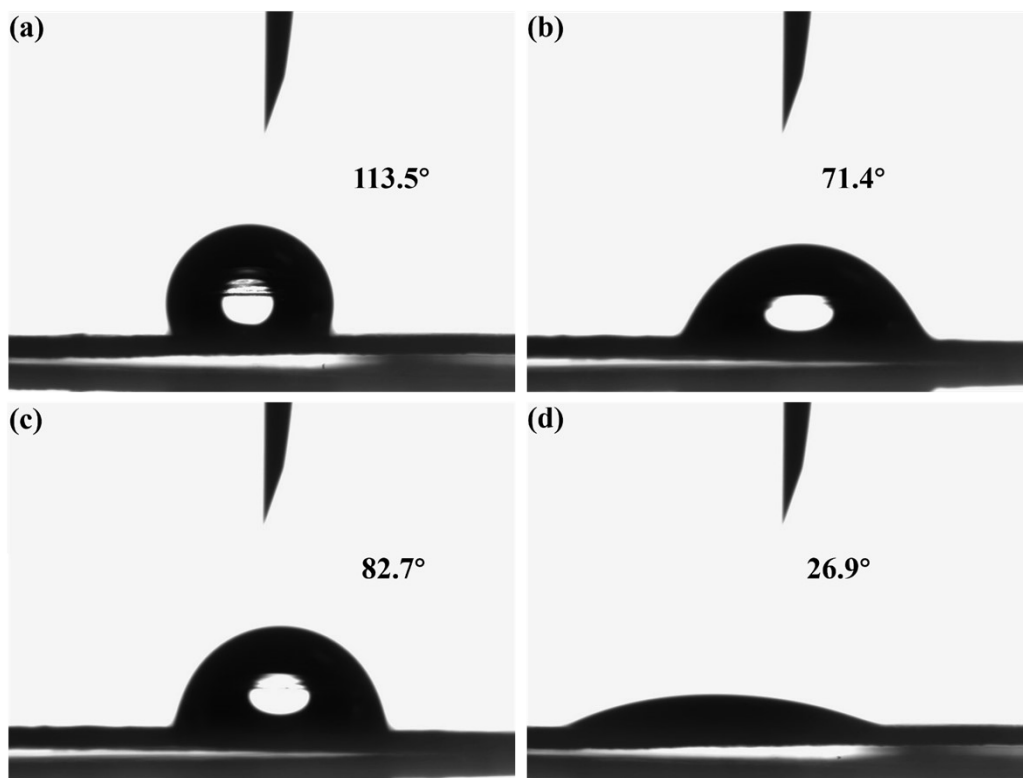


**Figure. S11** Contact angle of HMF solution on (a)Ni foam, (b) NiMoO<sub>4</sub>/NF, (c) NiNH/NF, and (d) N-NiMoO<sub>4</sub>/NF electrode surface.



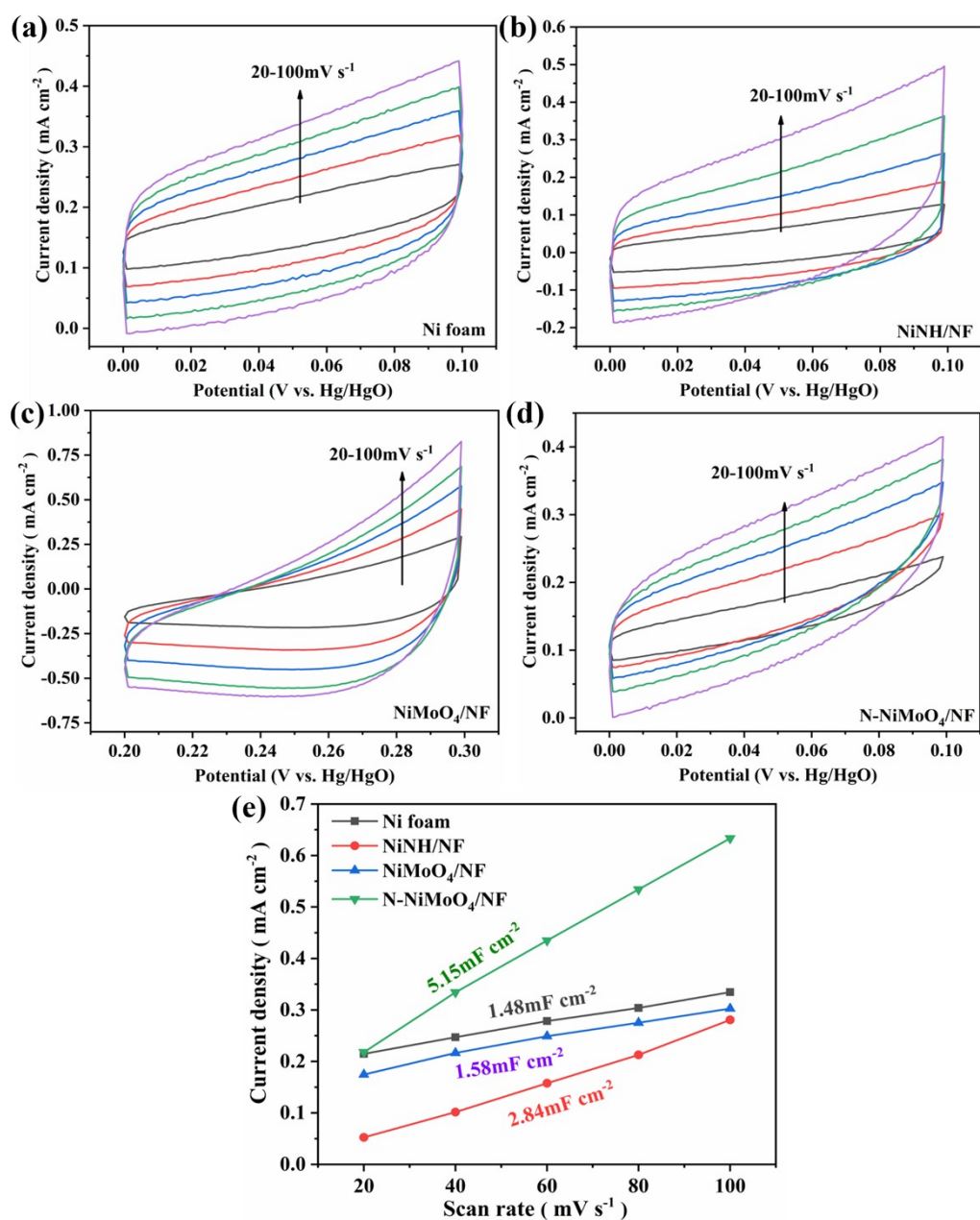


**Figure. S12** Cyclic voltammetry of (a) Ni foam , (b) NiNH/NF , (c) NiMoO<sub>4</sub>/NF , (d) N-NiMoO<sub>4</sub>/NF at the scanning rate of 20-100  $\text{mV s}^{-1}$ , (e) the relationship between current density and scanning rate

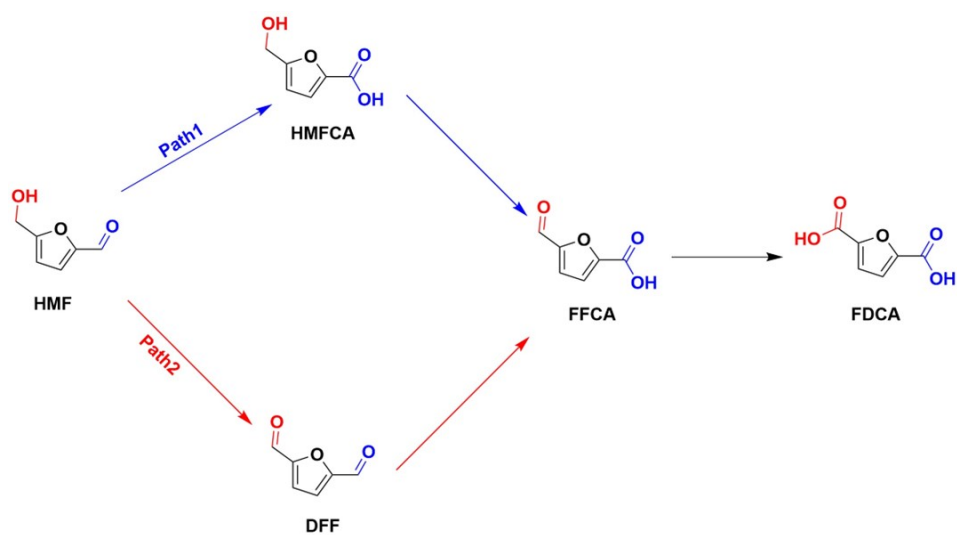


**Figure S13** Two possible pathways of converting HMF to FDCA.

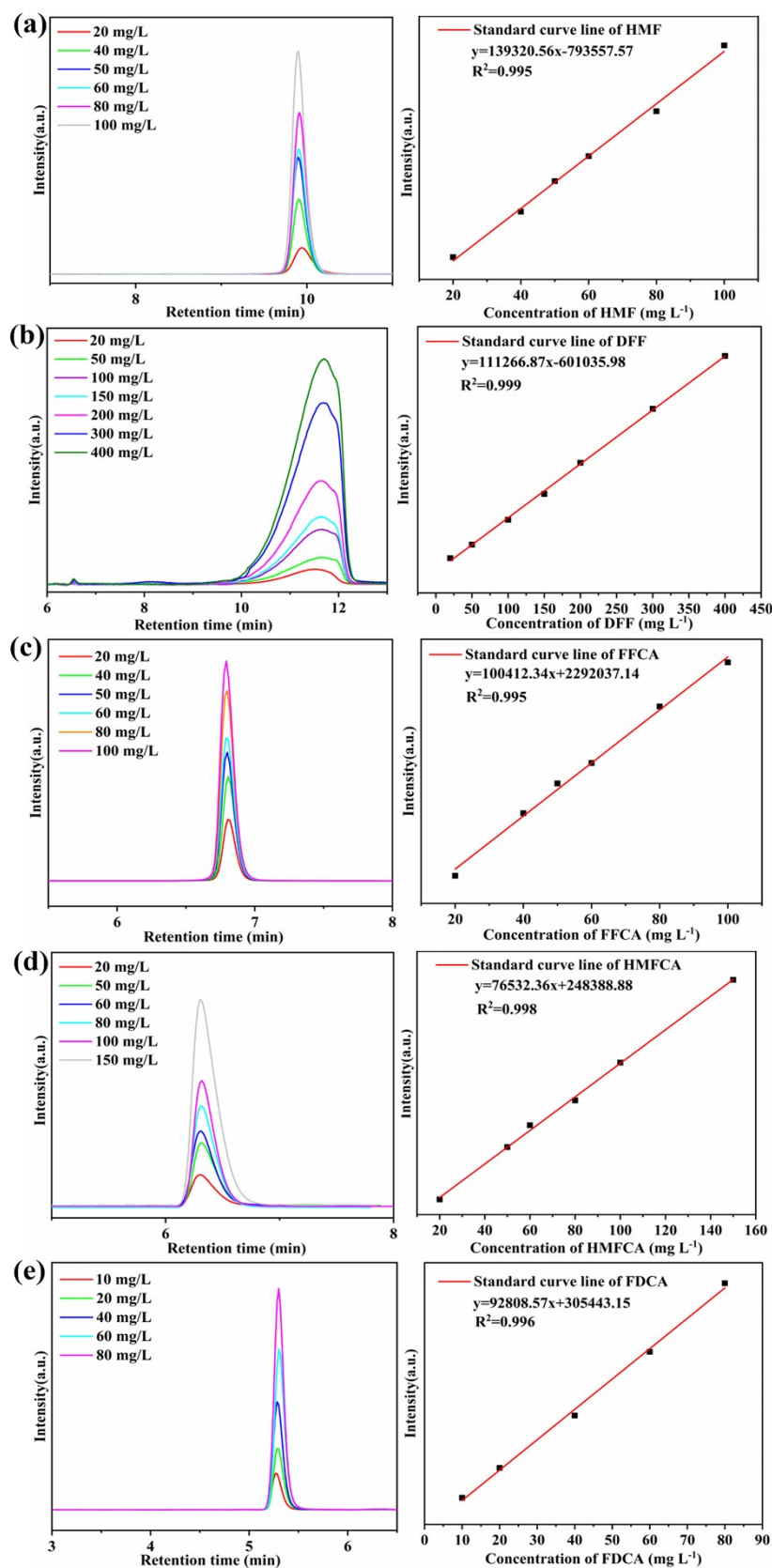


**Figure. S14** HPLC chromatogram of standard samples at different concentrations and standard curve: (a) HMF, (b) DFF, (c) FFCA, (d) HMFCA, and (e) FDCA.

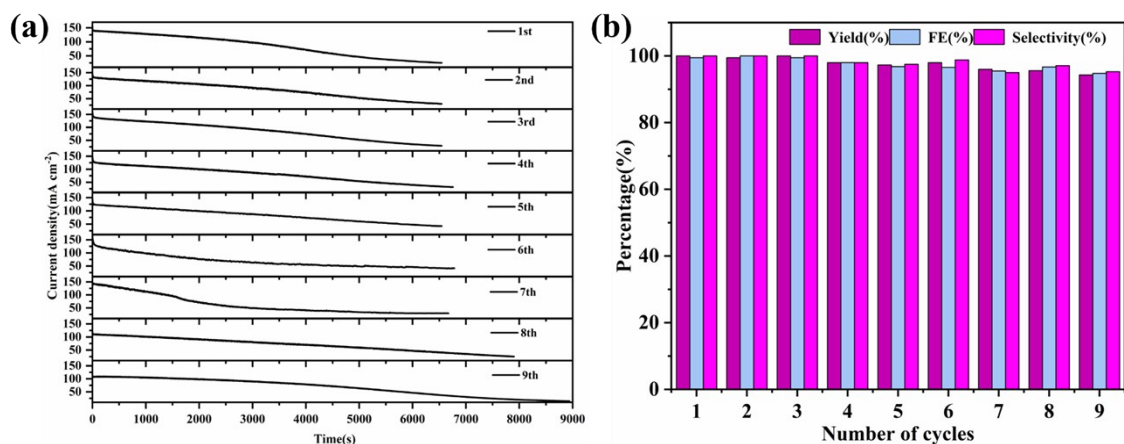


**Figure S15** N-NiMoO<sub>4</sub>/NF i-t curve lasting 9 cycles at 1.52 V (vs. RHE), (b) the yield, FE and selectivity at different cycle times.

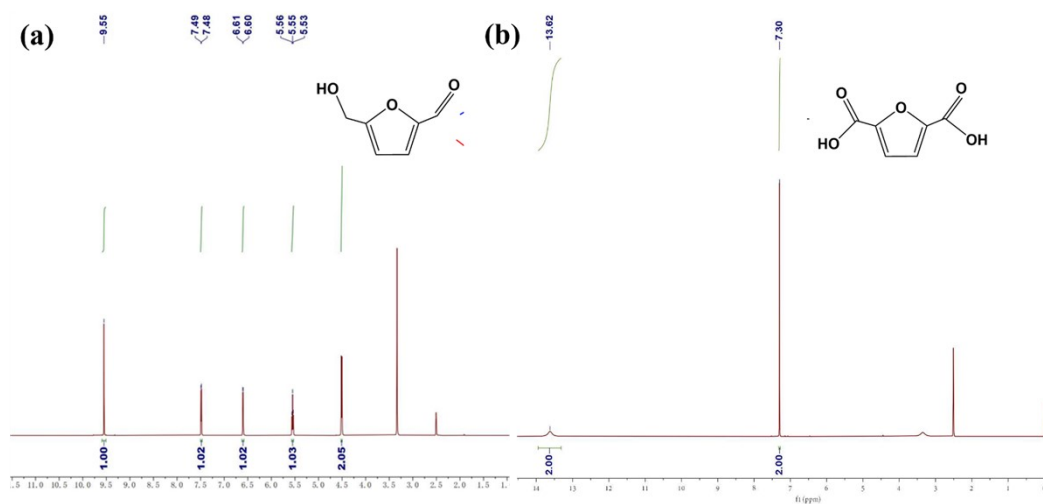


**Figure S16** (a) <sup>1</sup>H NMR spectra of HMF raw material, (c) <sup>1</sup>H NMR spectra of acid-precipitated solid products.

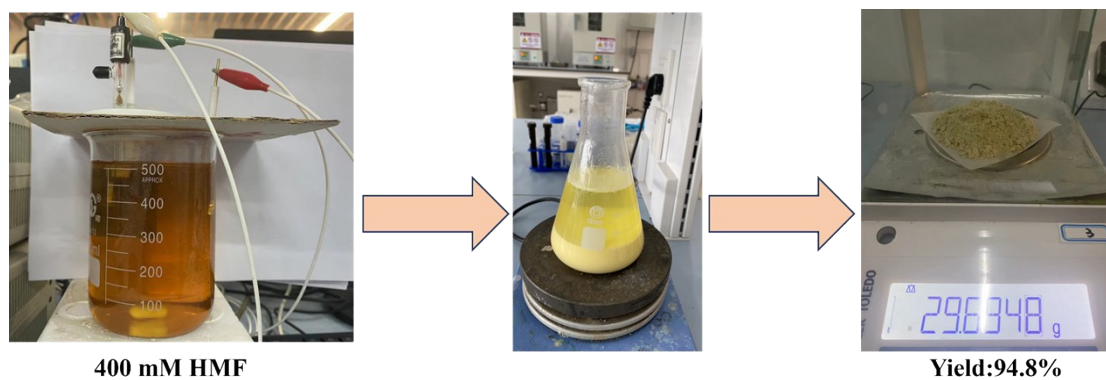


**Figure S17** Enlarge the actual picture of the experiment.

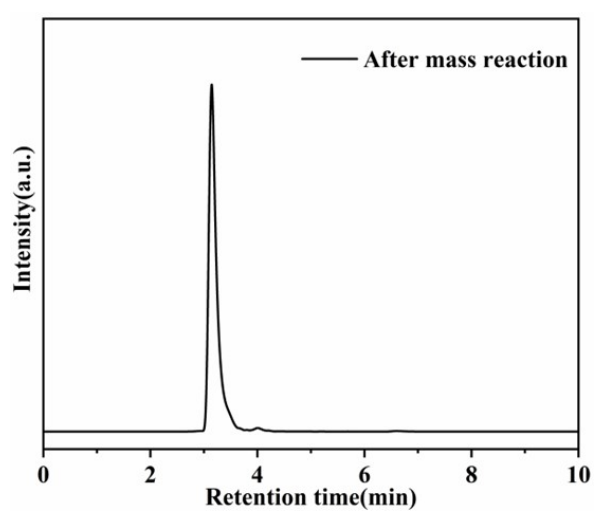


**Figure S18** HPLC diagram after magnification experiment.

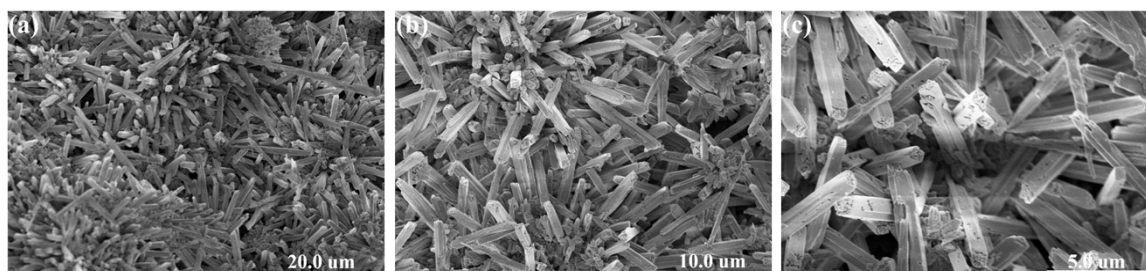


**Figure S19** SEM images for N-NiMoO<sub>4</sub>/NF after 3 i-t cycle tests.

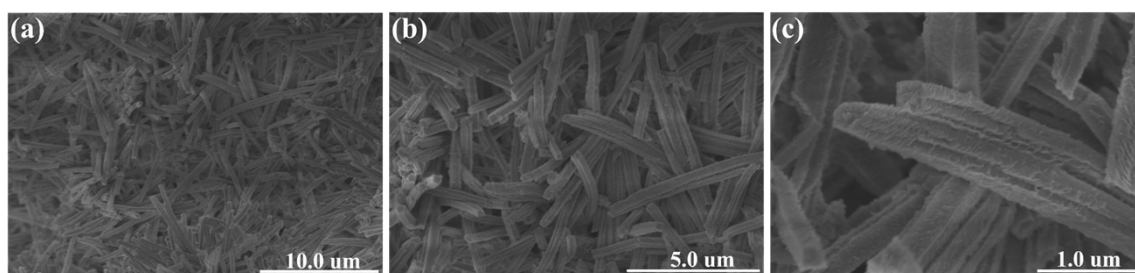


**Figure S20** SEM images for N-NiMoO<sub>4</sub>/NF after 9 i-t cycle tests.

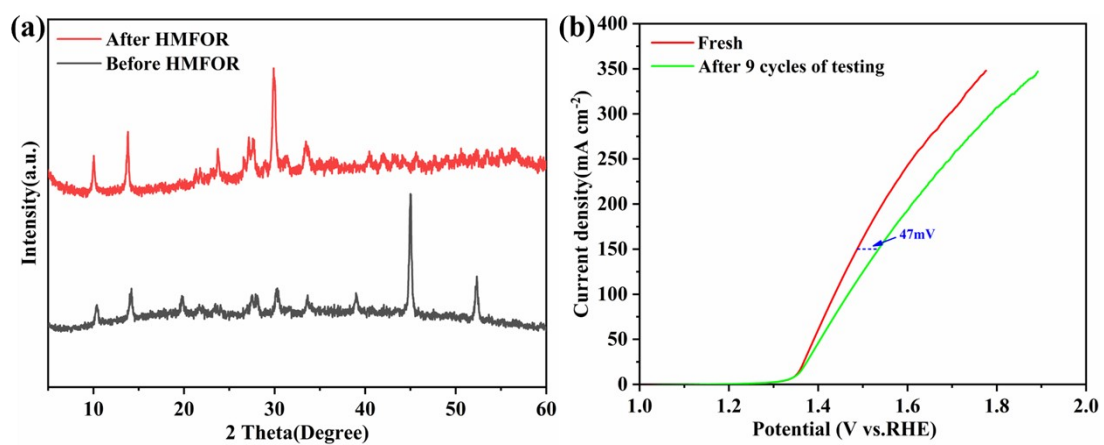


**Figure S21** (a) XRD pattern for N-NiMoO<sub>4</sub>/NF after 9 i-t cycle tests, (b) LSV curves before and after cyclic test of N-NiMoO<sub>4</sub>/NF.

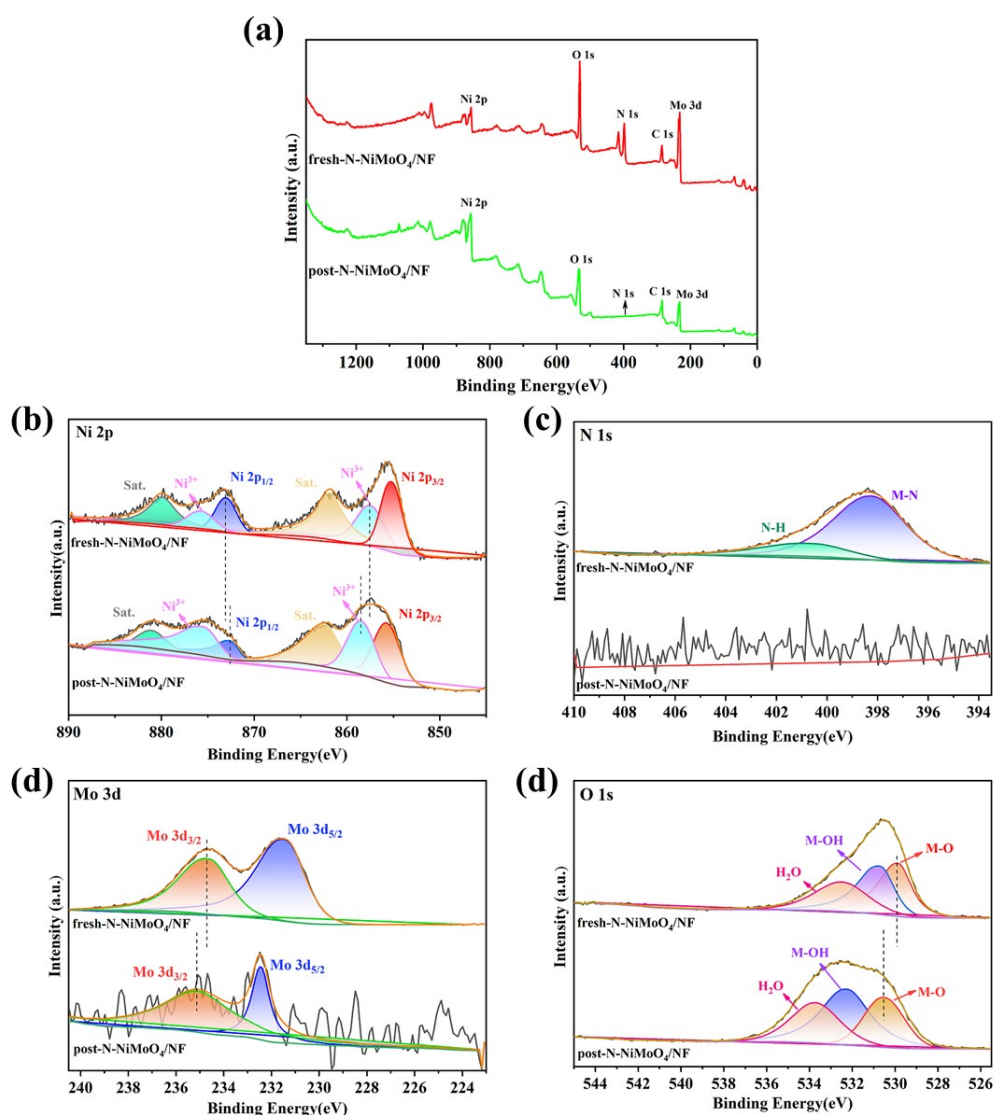


**Figure S22** High-resolution XPS spectra for (a) survey full spectra, (b) Ni 2p, (c) N 1s, (d) Mo 3d (e) O 1s before and after HMFOR.



**Table S1** Lattice parameters of NiMoO<sub>4</sub> and NiMoO<sub>4</sub>·H<sub>2</sub>O

Samples	$a$ (Å)	$b$ (Å)	$c$ (Å)	$\alpha$ (°)	$\beta$ (°)	$\gamma$ (°)	$V$ (Å <sup>3</sup> )	Space Group
NiMoO <sub>4</sub>	9.566	8.734	7.649	90.00	114.22	90.00	582.82	$C_{2/m}$
NiMoO <sub>4</sub> ·H <sub>2</sub> O	4.4700	6.9500	8.4100	76.60	84.20	74.50	244.71	$P_1$

**Table S2** Impedance fitting results of as-prepared N-NiMoO<sub>4</sub>/NF, NiMoO<sub>4</sub>/NF, NiNH/NF and Ni foam.

catalyst	$R_s/\Omega \text{ cm}^{-2}$	$R_{ct}/\Omega \text{ cm}^{-2}$
N-NiMoO <sub>4</sub> /NF	1.16	3.30
NiMoO <sub>4</sub> /NF	1.65	5.20
NiNH/NF	2.12	6.07
Ni foam	2.59	10.87

**Table S3** The electrocatalytic performance comparison of prepared N-NiMoO<sub>4</sub>/NF with reported HMFOR electrocatalysts.

Electrocatalysts	Potential(V vs.RHE)	HMF (mM)	Conversion (%)	FDCA yield (%)	FE (%)	Ref.
N-NiMoO <sub>4</sub>	1.473	10	100	97	97	<i>Catal. Sci. Technol.</i> 2021, 11, 7326-7330.
Co <sub>3</sub> O <sub>4</sub>	1.65	10	100	93.2	92.9	<i>Appl. Catal. B Environ.</i> 2022, 307, 121209.
NiOOH/Cu(OH) <sub>2</sub>	1.50	5	100	93.8	93.8	<i>ACS Catal.</i> 2022, 12, 4078-4091.
Ni/NiO heterostructures	1.45	50	95	91	95	<i>Catal. Sci. Technol.</i> 2021, 11, 2480-2490.
Ni(OH) <sub>2</sub> -1PO <sub>x</sub>	1.464	10	> 99	94.2	93.5	<i>ACS Sustainable Chem. Eng.</i> 2022, 10, 5538-5547.
NiB	1.45	10	> 99	98.5	100	<i>Angew. Chem. Int. Ed.</i> 2018, 57, 11460.
NCF (Cu foam)	1.62	5	99.9	96.4	95.3	<i>ACS Catal.</i> 2018, 8, 1197-1206.
Co <sub>3</sub> O <sub>4</sub> /CF	1.40	10	1.0 M KOH	92.9	93.2	<i>Appl. Catal. B-Environ.</i> <b>2022</b> , 307, 121209.
NiS <sub>x</sub> /β-Ni(OH) <sub>2</sub>	1.45	10	1.0 M KOH	98.3	97.7	<i>Adv. Mater.</i> <b>2023</b> , 35, 2211177
Ni <sub>3</sub> N@C	1.45	10	1.0 M KOH	99	98.0	<i>Angew. Chem.</i> <b>2019</b> , 131, 16042
Co <sub>0.4</sub> NiS@NF	1.45	10	1.0 M KOH	98.5	96.3	<i>Adv. Sci.</i> <b>2022</b> , 9, 2200957

Co-NiO/CC	1.47	10	1.0 M KOH	94.6	94.8	<i>Chem. Eng. J.</i> , <b>2022</b> , 433, 133842
NiOOH-VN/NF	1.402	10	1.0 M KOH	95.0	94.7	<i>Chem. Eng. J.</i> , <b>2022</b> , 433, 133842
Ni <sub>3</sub> S <sub>2</sub> -MoS <sub>2</sub>	1.45	10	1.0 M KOH	93.0	93.0	<i>Small</i> <b>2022</b> , 18, 2201306
NiRu@PCNS	1.45	10	1.0 M KOH	NA	98.2	<i>Chem. Eng.</i> <b>2023</b> , 11, 13441
Co <sub>4</sub> N/NC@CC	1.40	10	1.0 M KOH	90.3	92.4	<i>ACS Catal.</i> <b>2022</b> , 12, 4242
NiSe@NiO <sub>x</sub>	1.423	10	1.0 M KOH	95.0	93.0	<i>Appl. Catal B- Environ.</i> <b>2020</b> , 261, 118235
Al(OH) <sub>3</sub> /Co(OH) <sub>2</sub>	1.5	10	100	99.1	99.4	<i>Adv. Mater.</i> 2023, 35, 2301549
N-NiMoO <sub>4</sub> /NF	1.52	20	100	99.8	99.8	<b>This work</b>

